Acta Oceanol. Sin., 2020, Vol. 39, No. 6, P. 96–106
https://doi.org/10.1007/s13131-019-1470-y
http://www.hyxb.org.cn
E-mail: hyxbe@263.net

Detail description of *Lithophyllum okamurae* (Lithophylloideae, Corallinales), a widely distributed crustose coralline alga in marine ecosystems

Qunju Hu[1, 2], Fangfang Yang[1], Zhangliang Wei[1, 2], Jiahao Mo[1, 2], Chao Long[1, 2], Xinpeng Tian[1], Lijuan Long[1]*

[1] CAS Key Laboratory of Tropical Marine Bio-resources and Ecology, South China Sea Institute of Oceanology, Chinese Academy of Sciences, Guangzhou 510301, China

[2] University of Chinese Academy of Sciences, Beijing 100049, China

Received 3 January 2019; accepted 22 April 2019

Abstract

Lithophyllum okamurae is one of the important encrusting coralline algae, which plays important roles as primary producer, carbonate sediment builder, and habitat provider in the marine ecosystems. In this study, *L. okamurae* was collected from tropical coast of Sanya, and firstly described based on both detailed morph-anatomical characteristics and molecular studies of typic DNA sequences. The structure of the thalli of *L. okamurae* was pseudoparenchymatous construction with radially organized dimerous organizations in the crustose portion. The pseudoparenchymatous construction were composed of three parts, including 1 to 3 layers of epithelia cells which had flatten to round outermost walls, one layer of square or rectangular cells of the hypothallia and multiple layers of square or elongated rectangular peripheral cells. Palisade cells were observed, and the cells of the contiguous vegetative filaments were connected by secondary pit-connections with cell fusions absent. The carposporangial conceptacles, the spermatangial conceptacles, the bisporangial conceptacles and the tetrasporangial conceptacles were observed, and all these four kinds of conceptacles were uniporate. The spermatangial conceptacles were slightly convex and buried at shallow depths in the thalli tissues, and the carposporangial conceptacles and asexual conceptacles were protruding and conical. Phylogenetic studies based on DNA barcoding markers of 18S rDNA, COI, *rbc*L and *psb*A revealed that *L. okamurae* clustered with the closest relation of *L. atlanticum*, and formed a distinct branch. Based on the comparative anatomical features and the molecular data, the detailed description of the valid species of *L. okamurae* was firstly given in this study to provide theoretical basis for algae resources utilization and conservation in marine ecosystems.

Key words: *Lithophyllum okamurae*, crustose coralline algae, marine ecosystem, morphological characteristics, conceptacles, DNA-barcoding

Citation: Hu Qunju, Yang Fangfang, Wei Zhangliang, Mo Jiahao, Long Chao, Tian Xinpeng, Long Lijuan. 2020. Detail description of *Lithophyllum okamurae* (Lithophylloideae, Corallinales), a widely distributed crustose coralline alga in marine ecosystems. Acta Oceanologica Sinica, 39(6): 96–106, doi: 10.1007/s13131-019-1470-y

1 Introduction

Lithophyllum Philippi (1837: 387) is one of the currently recognized genera with living representatives in order Corallinales. It is a common non-geniculate rhodolith-forming genus of the subfamily Lithophylloideae Setchell (1943:134) (Harvey and Woelkerling, 2007; Li et al., 2018), which possess secondary pit connections and lack of genicula (Woelkerling, 1996; Harvey and Woelkerling, 2007). Species in *Lithophyllum* genus are known to form rhodoliths and commonly occur in marine environments such as coral reefs, rocky shores and rhodolith beds (Riosmena-Rodríguez et al., 1999; Harvey and Woelkerling, 2007). Species of genus *Lithophyllum* neither produce haustoria nor have thalli which are composed of flattened branches with isobilateral internal organizations (Woelkerling, 1996; Harvey and Woelkerling, 2007; Richards et al., 2014). Members of this genus are capable of building calcified concretions that cover large portions of rocky bottoms and other substrates (Xia, 2004; Li et al., 2018). Their critical roles in marine ecosystems are widely acknowledged, especially for their contributions to primary production, biodiversity repository and carbon burial (Nelson, 2009; McCoy and Kamenos, 2015; van der Heijden and Kamenos, 2015; Riosmena-Rodríguez et al., 2017).

Traditionally, classification of non-geniculate coralline is limited to morph-anatomical characters such as construction of the thalli, arrangement of basal filaments, cell fusions, conceptacle perforations, and the development of spores and gemmates (Woelkerling, 1983; Braga and Aguirre, 2004; Harvey et al., 2006; Harvey and Woelkerling, 2007; Villas-Boas et al., 2009; Kundal, 2011; Xia, 2004; Vieira-Pinto et al., 2014). However, non-geniculate coralline algae have also been regarded as highly morphologically variable, which depends on environmental conditions (Steneck, 1986; Woelkerling et al., 1993; Maneveldt et al., 2008).

Foundation item: The Strategic Priority Research Program of the Chinese Academy Sciences under contract No. XDA13020203; the Guangdong Science and Technology Project under contract No. 201707010174; the National Natural Science Foundation of China under contract No. 41806145.

*Corresponding author, E-mail: longlj@scsio.ac.cn

And it is both time consuming and technically challenging to decalcify non-geniculate coralline algae prior the detailed observation of anatomical features (Steneck, 1986; Woelkerling et al., 1993; Maneveldt et al., 2008; Nelson et al., 2015). All the above reasons make it difficult to classify non-geniculate coralline algae in the field by morph-anatomical features alone (Woelkerling, 1996; Nelson et al., 2015). Over the past decade, molecular phylogenetics has been developed as an increasingly accepted method for algal species identification (Maggs et al., 2007). And this method has been widely used to investigate accurate phylogeny of non-geniculate coralline algae, in which a range of genetic markers have been employed to unravel the relationships of them (Vieira-Pinto et al., 2014; Nelson et al., 2015; Rösler et al., 2016; Liu et al., 2018). The use of DNA sequence data as methods of identification become increasingly important in researches on systematic taxonomy, genetic diversity, population boundaries and connectivity of non-geniculate coralline algae (Rösler et al., 2016; Peña et al., 2018; Torrano-Silva et al., 2018). The use of DNA sequence data to assist with identification has both greatly aided taxonomic investigations, and also enabled the reliability of traditional taxonomic characters to be re-evaluated (Hajibabaei et al., 2007; Nelson et al., 2015). Therefore, it is crucial for accurate systematic evaluation of *Lithophyllum* species to combine detailed morph-anatomical characteristics and molecular DNA sequences (Vidal et al., 2003).

Lithophyllum okamurae is an abundant species of *Lithophyllum* genus, which is usually distributed in the pinkish-gray algal ridges at the windward reef bump band of the rocky coast in coral reef ecosystems (Xia, 2004; Ding et al., 2015; Phang et al., 2016; Li et al., 2018). Similar to the other non-geniculate coralline algae, *L. okamurae* has a triphasic life history, and it disperses mostly by spores (bispores/tetraspores and carpospores) (Chihara, 1974; Johansen, 1976; Verlaque, 2010). However, few studies regarding the descriptions of *L. okamurae* were available (Xia, 2004), especially on the DNA molecular taxonomic datasets. In this study, detailed descriptions of the morpho-anatomical features of *L. okamurae* were presented and four DNA molecular markers were used to determine the phylogenetic relations of this species to other species in *Lithophyllum* genus, including a portion of the nuclear-encoded 18S rDNA gene (LSU), the mitochondria-encoded gene COI, and two chloroplast-encoded genes *rbc*L and *psb*A. The aim of this study is to describe *L. okamurae* base on morphological, anatomical and molecular analyses, and to lay basis for algae resources conservation and utilization in the marine ecosystems.

2 Materials and methods

2.1 *Sample collection*

Samples were obtained at the shore of the Luhuitou Peninsula (18.216 7°–18.218 7°N, 109.482 6°–109.487 9°E) in the Sanya Bay, Hainan Island, China. The fragments of well-developed, healthy populations of *L. okamurae* with 3–10 cm^2 outer superficial area were carefully cut off from the substrate using a hammer and chisel via scuba diving at depths ranging from 1 m to 3 m in March, 2016. All the samples were placed in oxygenated transit cases filled with seawater and transported to the laboratory.

2.2 *Morphological and anatomical analysis*

For morphological observation, thalli of *L. okamurae* were observed and examined using a stereomicroscope (Stemi, 2000, Zeiss, Germany). For anatomical observation and measurements, thalli of *L. okamurae* were fixed in 4% formalin in seawater, and serial sections were prepared and stained with aniline blue after decalcification, dehydration and embedding step by step (Basso et al., 2004; Basso and Rodondi, 2006). Finally, the permanent slides were examined and photographed using a light microscope (BX53, Olympus, Japan) with a camera (Leica DMRB, Germany). For detail morphometrical observation and anatomical measurements, thalli of *L. okamurae* were air-dried and mounted on silver stubs using graphite conductive adhesive and coated with 10 nm of gold. The treated measurements were observed using a scanning electron microscope (SEM) (Hitachi S-3400N, Japan). The growth form of the specimen was characterized according to Woelkerling et al. (1993). Measurements of anatomical terminologies of were determined by the method described by Adey and Adey (1973) and Woelkerling (1988). The measurements of conceptacles and cells were measured according to the instructions adopted by Adey and Adey (1973) and Basso et al. (2004), respectively.

2.3 *Molecular phylogenetic analysis*

For molecular analysis, sample of *L. okamurae* was processed, and total genomic DNA was extracted using the eDNA HP Plant DNA Kit (Omega, USA), following the manufacturer's instructions. A total of four pairs of primers mentioned in Table 1 were used for PCR amplifications of the gene sequences of 18S rDNA, COI, *rbc*L and *psb*A, respectively. The 18S rDNA sequence was amplified with the primers and methods published by Harper and Saunders (2001). The COI was amplified with the primers published by Saunders (2005) and methods modified by Clarkston and Saunders (2010). The *rbc*L and *psb*A locus were amplified using the primers and protocols as Yoon et al. (2002). Purification and sequencing reactions were performed by BGI Genomics Co. Ltd., Shenzhen, China. The quality of the sequence data was verified by visual inspection of the electropherograms in Sequence Scanner 1.0 (Applied Biosystems, Waltham, MA, USA). Forward and reverse sequences were assembled by BioEdit version 5.0.6 (Hall, 1999), and chromatograms were checked to confirm the validity of ambiguous nucleotides. Multiple sequence alignments were performed for these gene sequences of 18S rDNA, COI, *rbc*L and *psb*A datasets using Clustal-W in Mega version 5 (Tamura et al., 2011), and phylogenetic datasets were constructed for each marker individually.

Phylogenetic analyses were performed using maximum likelihood (ML) and Bayesian (BA) methods. Maximum likelihood for all four sequences data were conducted in MEGA 5 using the Tamura-Nei model with 1 000 bootstrap replicates to assess branch support. Bayesian analyses were estimated using a Bayesian Markov chain Monte Carlo (MCMC) method implemented in BEAST package v1.8.0 (Drummond et al., 2005). The model used in these Bayesian analyses were general time reversible (GTR) substitution in which gamma distribution rate (G) and invariant sites (Γ4) was chosen on the basis of log likelihood (lnL) and Akaike's Information Criterion (AIC) scores inferred by Mr-Modeltest v2.3 (Nylander, 2004). Chains were conducted for 1×10^8 generations and sampled every 10 000 steps for each molecular clock model. Posterior probabilities were calculated using the software Tracer v. 1.6 after 10% burn-in. In all analyses, unrooted trees were calculated and the ingroup taxa subsequently rooted with *Phymatolithon* sp. as designated outgroup (Adey et al., 2015; Hernández-Kantún et al., 2016; Liu et al., 2018).

3 Results

Lithophyllum okamurae Foslie, 1900, p. 4; 1904, p. 59, p1s

Table 1. Four pairs of primers used to perform the sequences

Primer	Sequence	Reference
18S-G01	5′-CACCTGGTTGATCCTGCCAG-3′	Harper and Saunders (2001)
18S-G14	5′-CTTGGCAGACGCTTTCGCAG-3′	Harper and Saunders (2001)
COI-F	5′-TCAACAAATCATAAAGATATTGG-3′	Saunders (2005)
COI-R	5′-ACTTCTGGATGTCCAAAAAAYCA-3′	Saunders (2005)
*rbc*L-090F	5′-CCATATGCYAAAATGGGATATTGG-3′	Yoon et al. (2002)
R-*rbc*S start	5′-TGTGTTGCGGCCGCCCTTGTGTTAGTCTCAC-3′	Yoon et al. (2002)
*psb*A-F	5′-ATGACTGCTACTTTAGAAAGACG-3′	Yoon et al. (2002)
*psb*A-R2	5′-TCATGCATWACTTCCATACCTA-3′	Yoon et al. (2002)

11–19, Figs 11–19; 1929, p. 26, p1. 64, Figs 1–6; Dawson, 1954, p. 427, Fig. 39; Masaki and Tokida, 1963, p. 1, p1s 1–3; Masaki, 1968, p. 36, p1. 62, Fig. 6; Zhou and Zhang, 1985, p. 42, p1. III: 4, 5; 1991, p. 17; Lee, In Kyu and Jae, 1986, p. 320; Baba, 1987, p. 22, Figs 22–29, pls 9–11; Silva et al., 1987, p. 36; Silva et al., 1996, p. 249; Yoshida, 1998, p. 577, Figs 3–25 A–G; Woelkerling et al., 2005, p. 176, 178; Xia, 2004, p. 66, Figs 50–51; Guiry and Guiry, 2018.

Homotypic and heterotypic synonyms: *Lithophyllum okamurae* f. trincomaliense

Foslie 1906; *Lithophyllum okamurae* f. validum Foslie 1906; *Lithophyllum validum* (Foslie) Foslie 1909.

Type Locality: Marine Laboratory, Sagami Province (Kanagawa Prefecture), Japan (Woelkerling et al., 2005).

Geographic Distribution: *L. okamurae* occurs in the South-east Asia (Indonesia, Myanmar, Vietnam), South-west Asia (India, Sri Lanka, Israel, Saudi Arabia), Asia (China, Japan, Korea), Pacific Islands (Fiji, Republic of Palau, Solomon Islands), and the Indian Ocean islands (Xia, 2004; Ding et al., 2015; Phang et al., 2016; Guiry and Guiry, 2018).

Habitat and Phenology: Plants attached to rocks, shells and coral skeletons, in shallow water of lagoons (Xia, 2004).

3.1 *Morphological and anatomical analyses*

3.1.1 *Morphological analysis*

Plants of *L. okamurae* were non-geniculate and attached ventrally to the substratum, growth-form encrusting to warty to lumpy (Fig. 1a). Wart-like short branches crowded on the thalli surfaces were 4 to 8 mm in diameter and 5 to 10 mm in height, and they were usually combined with each other to form flat or depressed apexes (Fig. 1a). Color of the *L. okamurae* thalli ranged from grayish-purple to dark purple (Fig. 1a). The structure of the crustose portion was pseudoparenchymatous with dimerous organization which internally organization dorsiventral and usually crusted up to 500 to 10,000 μm thick (Fig. 1b). Based on the anatomical microscope images, apical growth of *L. okamurae* filaments produced visible growth bands (Fig. 1b). Color of the new tissues near the crust surfaces, the older tissues of deeper layered crusts and the oldest tissues of deepest parts of the crusts were greyish purple, yellow and white, respectively (Fig. 1b). On the surface view of the fertile thalli, conceptacles distributed on both the thalli surfaces and branches (Fig. 1c).

3.1.2 *Anatomical analysis*

The internal crustose parts of the thalli were pseudoparenchymatous construction with dimerous organization (Figs 1b and 2a). The construction of the crusts was composed of epithallium, hypothallium and the peripheral portions (Fig. 2a). The epithallium parts were composed of one to three layers of square or rectangular cells. The diameters in both transverse and longitudinal sections of the square cells were 4.0–7.0 μm, while the rectangular cells were 5.0–9.0 μm in diameter and 3.0–6.0 μm in height (Figs 2a, b). In view of surface, the polygonal epithallial cells were flat or had rim-like tops, and the outer peripheral parts of the epithallial cells with lost roofs were uncalcified (Fig. 2b). The hypothallium parts were composed of one layer of square or rectangular cells. The diameters in both transverse and longitudinal sections of the square cells were 7.0–13.0 μm, while the rectangular cells were 4.0–7.0 μm in diameter and 13.0–17.0 μm in height (Fig. 2a). The peripheral regions were composed of multiple layers of square or elongated rectangular cells. The square cells were 8.0–11.0 μm in diameters in both transverse and longitudinal sections, while the elongated rectangular cells were (5.0–) 7.0–8.0 (–10.0) μm in diameter and (10.0–) 12.0–17.0 (–23.0) μm in height (Figs 2a, c). In peripheral regions of the crusts, cells of adjacent filaments were joined only by secondary pit-connections, and cell fusions were absent (Fig. 2c). The palisade cells were observed, which were significantly taller than the width (Fig. 2d). As intracellular storage polymers, floridean starch grains were commonly found in the peripheral cells, but they were absent in the epithallium cells (Figs 2a, d). Calcium carbonate was deposited in the cell walls, while outer peripheral parts of the epithallium cells were uncalcified (Figs 2b, c). Calcium carbonate was orderly arranged in the cell walls (Fig. 2c). Periodical epithallium sloughing (synchronous epithallium shedding) was commonly observed in *L. okamurae*, which was epithallium cells flaked off

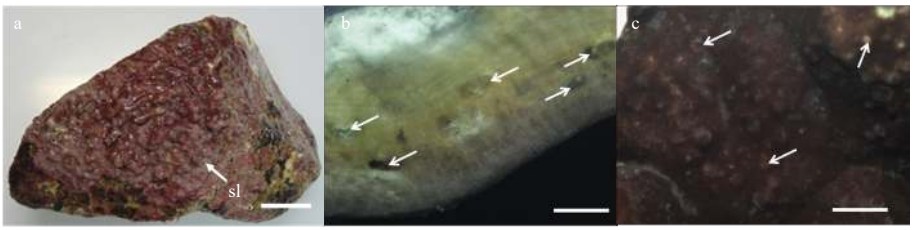

Fig. 1. Vegetative structures of *Lithophyllum okamurae*. a. External morphology of alga individuals growing on rocks, and sloughing cells (sl) in sheets form residual on the crust (white arrow). Scale bar is 3 cm. b. Cross-section showing the pseudoparenchymatous construction of the alga thallus, and conceptacles (white arrow) in it. Scale bar is 5 mm. c. Surface view of the thallus, showing conceptacles (white arrow) distributed on both surface and branches. Scale bar is 5 mm.

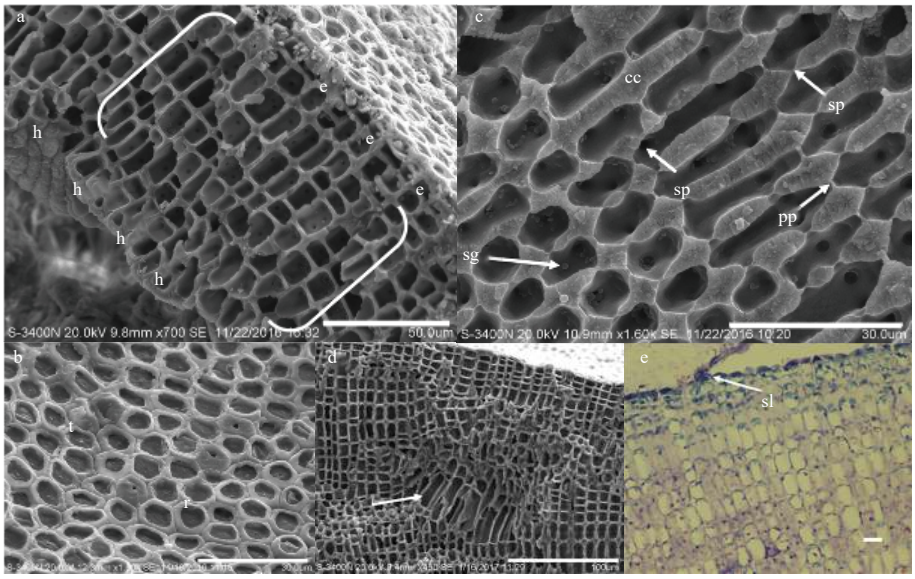

Fig. 2. Anatomical features of *Lithophyllum okamurae*. a. Vertical fracture showing the thallus crust with dimerous organization, and unistratose hypothallium (h), perithallium (bracket) and epithallium (e) visible. Scale bar is 50 μm. b. Surface view of polygonal epithallial cells with intact (t) and lost (r) roofs. The outer peripheral parts of epithallial cells with lost roofs were uncalcified. Scale bar is 30 μm. c. Vertical fracture showing primary pit connections (pp) and secondary pit connections (sp) among the filaments in peripheral region of the crusts, and calcium carbonate (cc) deposited in the cell walls, and floridean starch grains (sg) stored in the perithallium cells. Scale bar is 30 μm. d. Palisade cells (white arrow) in perithallium part of the crust. Scale bar is 100 μm. e. Epithallium cells sloughing (sl) in form of face peeling under optical microscope. Scale bar is 10 μm.

as large sheets of cells (Figs 1a and 2e). These sheets were white, thin and extensive on the thalli surfaces (Fig. 1a). During the sloughing process, the outer walls of the newly formed epithallium cells were ruptured and shed together with the sloughing epithallium cells (Fig. 2e).

3.1.3 *Reproductive structures*

In this study, the color of the conceptacles which buried in the crusts of *L. okamurae* was translucent or white (Fig. 1b). Gametangial thalli of *L. okamurae* were dioecious (Figs 3a, d). Uniporate conceptacles were mainly immersed in the perithallus region at both the thalli crusts and branches, and the unburied conceptacles were flushed with the thalli surfaces or raised (Figs 1c and 3a, d, g, h). There were four types of conceptacles, including the spermatangial conceptacles (Figs 3b, c), cystocarpic conceptacles (Figs 3e, f), bisporangial conceptacles (Figs 3j, l) and tetrasporangial conceptacles (Figs 3k, m, n) in *L. okamurae*. For the cystocarpic conceptacles and the asexual conceptacles (including the bisporangial conceptacles and tetrasporangial conceptacles), columellae were located in central of the conceptacle chambers (Figs 3d, g). In the asexual conceptacles, pores were formed by breakdown of upper parts of the columellae (Figs 3j–n). The spermatangial conceptacles were slightly convex, and usually shallow buried in the thalli tissues (Fig. 3a). The chambers of the spermatangial conceptacles were (123.0–) 138.0–163.0 (–175.0) μm in diameter in the longitudinal sections, and (38.0–) 53.0–63.0 (–80.0) μm in height in the transverse sections (Figs 3a, b, c). The spermatangia were numerous, small and narrowly cylindrical, which stood only on the chamber floors (Figs 3b, c). The spermatangia were 10.5–12.5 (–14.1) μm in length and (2.6–) 3.1–3.7 (–4.1) μm in diameter (Figs 3b, c). The cystocarpic conceptacles were submerged in the crusts, with their chambers 82.0–112.0 (–131.0) μm in height and (159.6–) 167.5–201.5 (–223) μm in diameter (Figs 3d, e, f). The carpogonia were in egg form, which were 19.3–26.0 μm in the longitudinal sections and 11.3–17.5 μm in the transverse sections (Figs 3e, f). The asexual conceptacles were flattened mound-like structures (Fig. 3h), whose chambers were buried in the crusts (Figs 3g, i), and the chambers were elliptical with steepled topped roofs (Fig. 3h). The height and diameter of the chambers of these asexual conceptacles were (100.0–) 125.0–150.0 μm and (170.0–) 240.0–265.0 (–315.0) μm, respectively. The columellae at the central parts of these asexual conceptacle chambers were formed by the upheaved chamber floors which crowned with hair cells (Figs 3j, n). Bisporangia and tetrasporangia were developed and arranged around the prominent central columellae in the bisporangial conceptacle and tetrasporangial conceptacle chambers, respectively (Figs 3l, m). The bisporangia were bipartite and stood on the periphery of conceptacle floors with long egg form with 39.0–73.2 μm in length and 16.8–28.5 μm in diameter (Figs 3j, l). The tetrasporangia were tetrad and stood on the periphery of conceptacle floors. They were also in long egg form with 39.6–52.8 μm in length and 9.9–23.1 μm in diameter, respectively (Figs 3k, m). The spermatangia (Fig. 3b), carpogonia (Fig. 3f), bisporangia (Fig. 3j) and tetrasporangia (Fig. 3n) were all released through the pores of the conceptacle chambers.

3.2 *Phylogenetic analyses*

In this study, all the four primers were successfully amplified for *L. okamurae*. Overall, an 805 base-pair portion of the 18S rDNA sequence, a 669 base-pair portion of the COI sequence, a 1 437 base-pair portion of the *rbc*L sequence, and a 901 base-pair portion of the *psb*A sequence of this alga were generated, respectively. All these sequences had been deposited in GenBank (18S rDNA: MH663996; COI: MH823811; *rbc*L: MH788639; *psb*A: MH788638). However, the amplified COI sequence was a NUMTs (nuclear mitochondrial DNA), and there were four terminator codes in it.

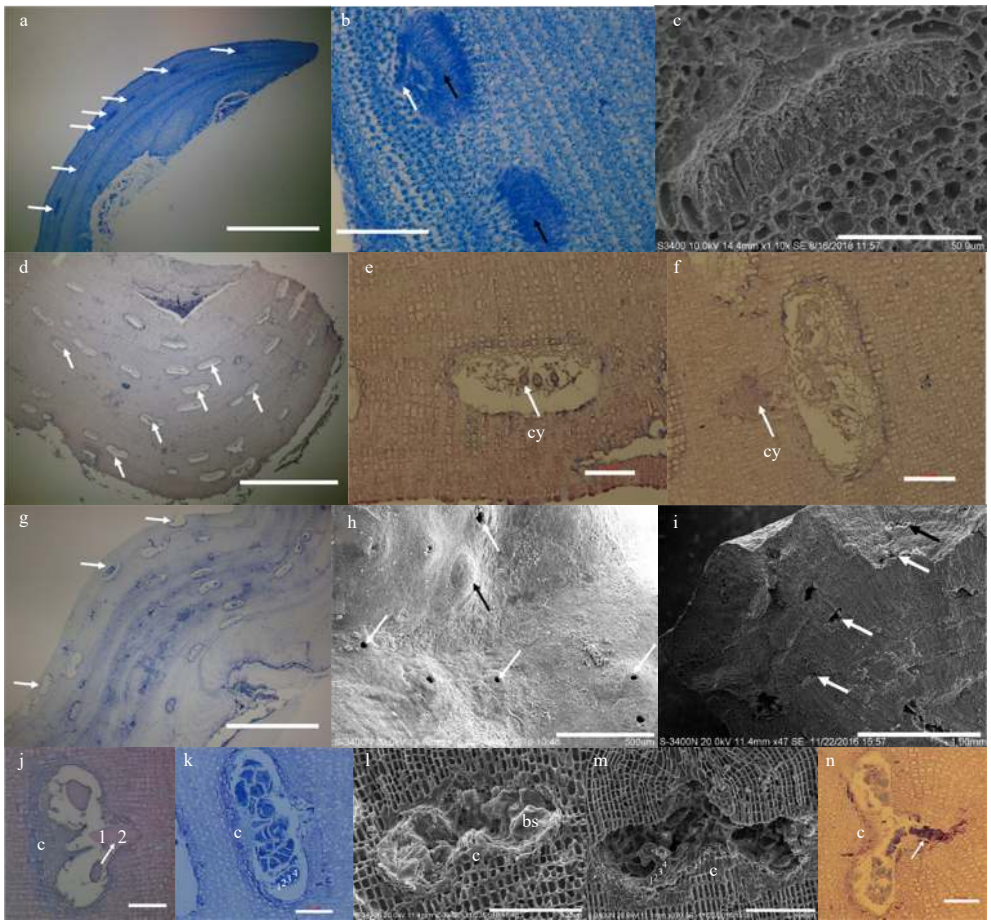

Fig. 3. Anatomical features of fertile crusts and the conceptacles of *Lithophyllum okamurae*. a. Cross section through a male plant showing spermatangial conceptacles (white arrow) of different developing stages. Scale bar is 1 mm. b. Two spermatangial conceptacles showing apical oblique divisions forming spermatangia (white arrow), and the spermatangia were releasing from the pore (black arrow). Scale bar is 100 μm. c. A spermatangial conceptacle in elder production stage, where spermatangia were produced on the floor of the conceptacle chamber. Scale bar is 50 μm. d. Cross section through a female plant showing cystocarpic conceptacles (white arrow) of different developing stages. Scale bar is 1 mm. e. A developing cystocarpic conceptacle with several cystocarps (cy) in the chamber. Scale bar is 50 μm. f. A cystocarpic conceptacle which was releasing its cystocarps (cy). Scale bar is 50 μm. g. Cross section through an asexual plant showing tetrasporangial or bisporangial conceptacles (white arrow). Scale bar is 1 mm. h. Surface view of a fertile thallus showing uniporate (white arrow) conceptacles, and a uniporate conceptacle with steepled topped roofs (black arrow). Scale bar is 500 μm. i. A fertile tetrasporophyte thalli with a bisporangial conceptacle (black arrow) and several tetrasporangial conceptacles (white arrow) originated in the crust. Scale bar is 1 mm. j. A bisporangial conceptacle with zonate bisporangia (white arrow) and central columella (c) in the chamber, with the bisporangia was releasing. Scale bar is 50 μm. k. A tetrasporangial conceptacle with zonate bisporangia (white arrow) and central columella (c) in the chamber. Scale bar is 50 μm. l. A bisporangial conceptacle with roof and showing putative zonately arranged bisporangia (bs), and the bisporangia arranged around a prominent central columella. Scale bar is 100 μm. m. A tetrasporangial conceptacle with roof showing putative zonately arranged tetrasporangia, and the tetrasporangia arranged around a prominent central columella (c). Scale bar is 100 μm. n. A tetrasporangial conceptacle which was releasing its tetrasporangia. Scale bar is 50 μm.

The final alignment for 18S rDNA consisted of 34 taxa, including the new sequence and 33 previously published coralline algae sequences, and the final dataset was a 765 base-pair portion of the 18S rDNA gene in the nuclear genome. The alignment for COI was composed of 37 taxa, including the new sequence and 36 GenBank sequences, and the final dataset was a 551 base-pair portion of the COI gene in the mitochondria genome. The alignment for *rbc*L consisted of 36 taxa, including the new sequence and 35 GenBank sequences, and the final dataset was a 630 base-pair portion of the *rbc*L gene in the plastid genome. The alignment for *psb*A was composed of 77 taxa, including the new sequence and 76 previously published sequences, and the final dataset was a 732 base-pair portion of the *psb*A gene in the plastid genome. For each of the sequence datasets, one ML tree and one BA tree were generated by bootstrap results from the distance analyses and Bayesian inference with posterior probabilities, respectively. A total of eight trees were generated in this study, and the topologies of the ML and BA trees were largely congruent. Then the ML trees were generated by both the bootstrap results and Bayesian inference for the sequence data (Fig. 4, Fig. S1, Fig. 5, Fig. S2). The ML trees for the COI (Fig. S1) and *psb*A (Fig. S2) sequence datasets, and the BA trees for the 18S rDNA (Fig. S3), COI (Fig. S4), *rbc*L (Fig. S5) and *psb*A (Fig. S6) sequence datasets were in supplement materials. And in all phylogenetic reconstructions, ambiguities were observed among *L. okamurae* and the other specimens of genus *Lithophyllum*.

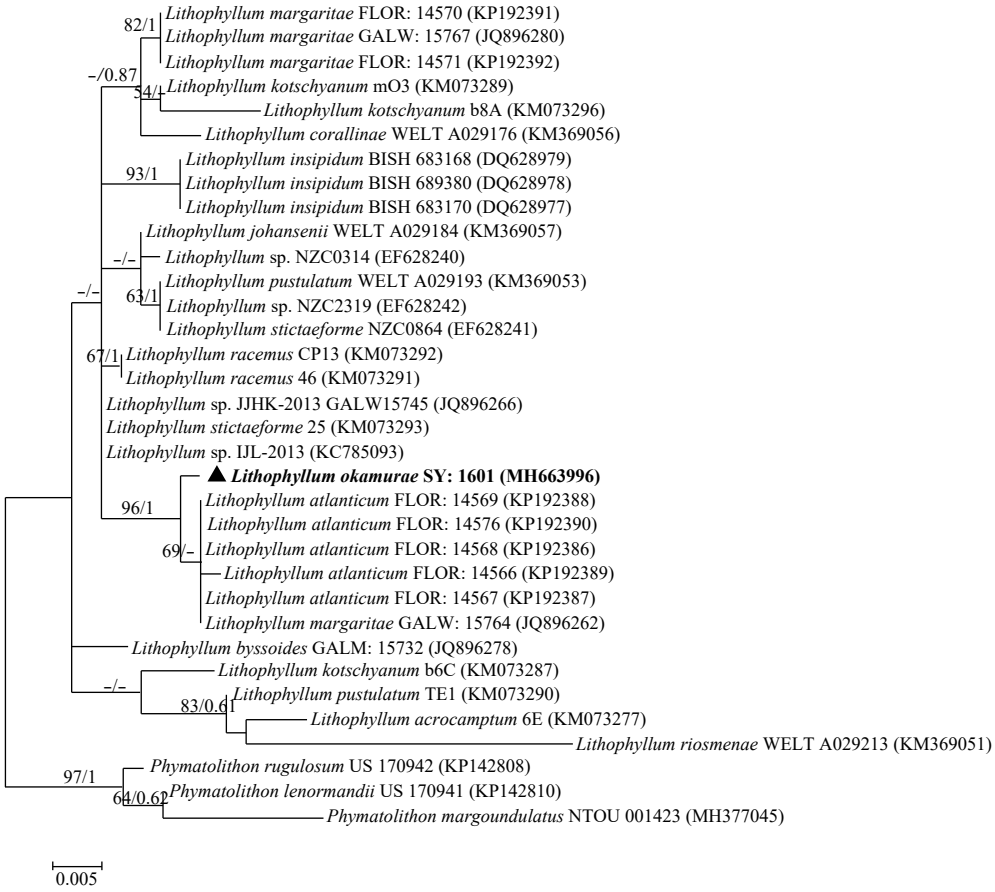

Fig. 4. Tree constructed with ML for the 18S rDNA alignment. Values at branches represent distance analyses of 1 000 bootstrap replicates (left value) and Bayesian posterior probabilities (right value). Branches lacking values received <50% support. GenBank accession numbers provided. The newly generated sequence was shown in bold.

3.2.1 *Phylogenetic relationships of Lithophyllum species based on nuclear 18S rDNA sequence data*

One 18S rDNA sequence was newly determined for this study. A phylogenetic tree was generated by bootstrap results from the distance and Bayesian inference with posterior probabilities (Fig. 4). The genus *Lithophyllum* was monophyletic with strong support (97% in bootstrap support and 1 in posterior probabilities). There were 19 well-supported monophyletic clades among the included *Lithophyllum* spp. was resolved based on our analyses, including 16 taxa described *Lithophyllum* spp. and 4 indeterminate known specific name specimens (Fig. 4). The 18S rDNA sequence of *L. okamurae* showed interspecific variation among the *Lithophyllum* species in these analyses ranged from 3 to 49 bp (0.4%–6.1%), and it showed interspecific variation with *L. atlanticum* sequences ranged from 3 to 5 bp (0.4%–0.67%). The single species of *L. okamurae* comprised a monophyletic lineage, which was strongly allied to the distinct clade of *L. atlanticum* from Brazil and *L. margaritae* from Mexico (96% in bootstrap support and 1 in posterior probabilities). And it was remotely related with the other clades of genus *Lithophyllum*. The species of *L. okamurae* formed an individual clade with full support.

3.2.2 *Phylogenetic relationships of Lithophyllum species based on nuclear COI sequence data*

One COI sequence was newly determined for this study. A phylogenetic tree was generated by bootstrap results from the distance and Bayesian inference with posterior probabilities (Fig. S1). The genus *Lithophyllum* was monophyletic with strong support (95% in bootstrap support and 1 in posterior probabilities). The analyses showed 14 monophyletic clades among the *Lithophyllum* spp., including 13 taxa described *Lithophyllum* spp. and 9 indeterminate known specific name specimens (Fig. S1). According to the results, COI sequence of *L. okamurae* showed interspecific variation among the *Lithophyllum* species in these analyses ranged from 46 to 95 bp (7.1%–14.6%), and it showed interspecific variation with the *L. atlanticum* sequences ranged from 46 to 47 bp (7.1%–7.3%). The single species of *L. okamurae* comprised a monophyletic lineage, which was moderately allied to the distinct clade of *L. atlanticum* from Brazil (52% in bootstrap support) and highly allied to the distinct clade of *Lithophyllum* sp. LAF7219 from Panama (96% in bootstrap support and 1 in posterior probabilities). The position of *L. okamurae* from the species of *L. atlanticum* from Brazil and *Lithophyllum* sp. LAF7219 was similar to that of the 18S rDNA reconstruction shown in Fig. 4, and *L. okamurae* formed an individual clade with full support.

3.2.3 *Phylogenetic relationships of Lithophyllum species based on nuclear rbcLsequence data*

One *rbc*L sequence was newly determined for this study. A phylogenetic tree was generated by bootstrap results from the distance and Bayesian inference with posterior probabilities (Fig. 5). The genus *Lithophyllum* was monophyletic with strong support (100% in bootstrap support and 1 in posterior probabilities). The

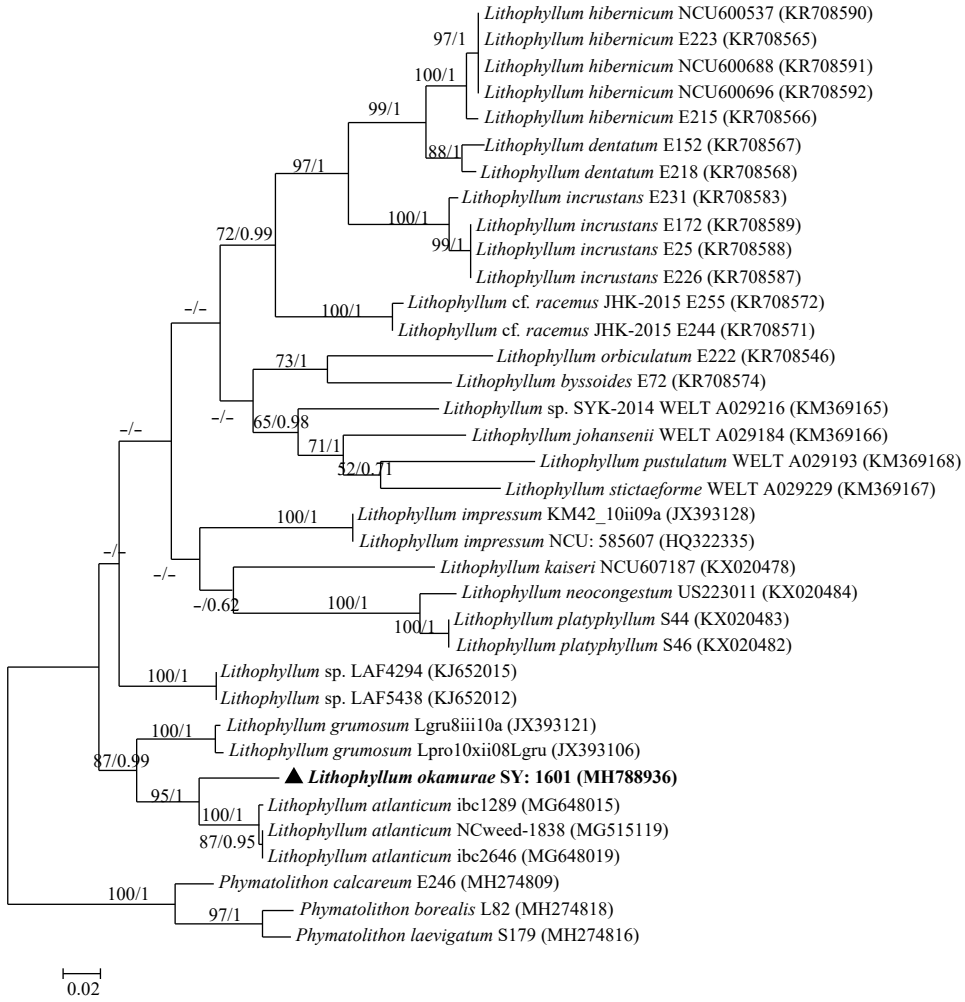

Fig. 5. Tree constructed with ML for the *rbc*L alignment. Values at branches represent distance analyses of 1 000 bootstrap replicates (left value) and Bayesian posterior probabilities (right value). Branches lacking values received <50% support. GenBank accession numbers provided. The newly generated sequence was shown in bold.

analyses showed 17 monophyletic clades among the *Lithophyllum* spp., including 16 taxa described *Lithophyllum* spp. and 9 indeterminate known specific name specimens (Fig. 5). According to the results, the *rbc*L sequence of *L. okamurae* showed interspecific variation among the *Lithophyllum* species in this analysis ranged from 90 to 210 bp (6.6%–15.7%), and it showed interspecific variation with the *L. atlanticum* sequences ranged from 90 to 112 bp (6.6%–8.2%). The single species of *L. okamurae* comprised a monophyletic lineage, which was highly allied to the distinct clade of *L. atlanticum* from Brazil (95% in bootstrap support and 1 in posterior probabilities). The position of *L. okamurae* from the clade of *L. atlanticum* from Brazil was similar to that of the 18S rDNA and COI reconstructions shown in Fig. 4 and Fig. S1, and *L. okamurae* formed an individual clade with full support.

3.2.4 *Phylogenetic relationships of Lithophyllum species based on nuclear psbA sequence data*

One *psb*A sequence was newly determined for this study. A phylogenetic tree was generated by bootstrap results from the distance and Bayesian inference with posterior probabilities (Fig. S2). The genus *Lithophyllum* was monophyletic with strong support (99% in bootstrap support and 1 in posterior probabilities). The analyses showed 25 monophyletic clades among the *Lithophyllum* spp., including 26 taxa described *Lithophyllum* spp. and 12 indeterminate known specific name specimens (Fig. S2). According to the results, the *psb*A sequence of *L. okamurae* showed interspecific variation among the *Lithophyllum* species in this analysis ranged from 23 to 108 bp (2.6%–12.6%), and it showed interspecific variation with the *Lithophyllum* sp. LAF7219 (Panama) and *L. margaritae* (Mexico) of 23 bp. Based on the *psb*A phylogram results, individual of *L. okamurae* specimen comprised a monophyletic lineage, which was moderately allied to the distinct clade of *L. margaritae* from Mexico (59% in bootstrap support). The clade of *L. okamurae* was separated from the specimens identified as *L. atlanticum* (Brazil) with branching order of ML distance value equalling 70% and posterior probabilities equalling 0.8, and highly allied to the distinct clade of *Lithophyllum* sp. LAF7219 (Panama) (94% in bootstrap support and 1 in posterior probabilities). The position of *L. okamurae* from the species of *L. margaritae* from Mexico, *L. atlanticum* from Brazil and *Lithophyllum* sp. LAF7219 from Panama was similar to that of the 18S rDNA, COI and *rbc*L reconstruction shown in Fig. 4, Fig. S1 and Fig. 5, and *L. okamurae* formed an individual clade with full support.

4 Discussion

Plant morpho-anatomical characteristics of *L. okamurae* re-

Table 2. Comparison of species in genus *Lithophyllum* that share characteristics with *Lithophyllum okamurae* (present study)

	L. okamurae (present study)	*L. atlanticum* (1)	*L. margaritae* (1)	*L. incrustans* (2)	*L. incrassatum* (2)	*L. neoatalayense* (2)	*L. corallinae* (3)	*L. kotschyanum* (3)	*L. neofarlowii* (3)	*L. pygmaeum* (3)	*L. yessoense* (3)
Substratum	rocks, corals and shells	free living and on rocks	free living	rocks and debris	rocks	rocks or spongites	growing on *Corallina* spp.	growing on corals	rocks	ND	ND
Epithallium											
Layer	1–3	1–2		1–4	1	⩾5	1	1		1	3–5
Diameter/μm	4.0–7.0/5.0–9.0	3.0–6.0	5.0–13.0	3.0–4.0	5.0–12.0	4.0–6.0	6.6–8.0	5.0–7.0		5.0–10.0	6.6–8.0
Length/μm	4.0–7.0/3.0–6.0	6.0–11.0	1.5–5.0	3.0–4.0	3.0–5.0	2.0–5.0	3.3–5.0	3.0–5.0		4.0–7.0	3.3–5.0
Hypothallium											
Layer	1						1	ND	2–3		1
Diameter/μm	7.0–13.0/4.0–7.0	5.5–11.0	3.0–10.0	12.0–15.0	9.0–22.0	6.0–15.0	6.9–9.9	7.0–10.0/5.0–10.0	5.0–6.0	5.0–7.0/5.0–10.0	6.6–9.9
Length/μm	7.0–13.0/13.0–17.0	8.0–17.0	7.0–16.0	9.0–11.0	9.0–22.0	3.0–10.0	19.8–23.1(–30.0)	7.0–10.0/7.0–20.0	10.0–13.2	5.0–7.0/7.0–23.0	5.0–6.6
Peripheral											
Diameter/μm	8.0–11.0/(5.0–)7.0–8.0 (–10.0)	4.5–10.0	4.0–8.0	3.0–35.0	6.0–12.0	9.0–11.0	6.6–9.9	5.0–13.0	3.3–5.0	8.0–16.0 (–23.0)/6.0–13.0	5.0–7.0
Length/μm	8.0–11.0/(10.0–) 12.0–17.0 (–23.0)	6.5–13.0	4.0–13.0	3.0–9.0	6.0–13.0	9.0–11.0	16.5–26.4	(13.0–)15.0–30.0 (–36.0)	6.6–9.9	35.0–60.0/7.0–22.0	5.0–8.0
Spermatangial											
Chamber diameter/μm *n*=15	(123.0–) 138.0–163.0 (–175.0)				156.0–269.0	130.0–221.0	72.6–89.1		125.4–224.5		
Chamber height/μm	(38.0–) 52.5–62.5 (–80.0)				33.0–52.0	39.0–73.0	42.9–52.8		33.0–46.2		
Spermatangia											
Diameter/μm *n*=15	(2.6–)3.1–3.7(–4.1)										
Length/μm	10.5–12.5(–14.1)										
Carposporangial conceptacles											
Chamber diameter/μm *n*=20	(159.6–) 167.5–201.5 (–223.0)						132.0–148.5				
Chamber height/μm	82.0–112.0 (–131.0)						66.0–108.9				
Carposporangia											
Diameter *n*=15	19.3–26.0						23.1–29.7				
Length	11.3–17.5						13.2–23.1				
Asexual conceptacles											
Chamber diameter/μm *n*=20	(170.0–) 240.0–265.0 (–315.0)	315.0–345.0	180.0–220.0	260.0–350.0	208.0–364.0	229.0–252.0	168.3–198.0	270.0–360.0	125.4–165.0	220.0–300.0	138.6–141.9
Chamber height/μm	(100.0–)125.0–150.0	90.0–130.0	70.0–95.0	110.0	52.0–130.0	83.0–177.0	99.0–105.6		79.2–105.6	75.0–130.0	66.0–112.2
Tetra/Bisporangia											
Diameter *n*=15	9.9–23.1(–28.5)	15.0–33.0	15.0–35.0	20.0–35.0	27.0–38.0	26.0–34.0	16.5–26.4	25.0–33.0	16.5–19.8	26.0–34.0	13.2–36.3
Length	(39.0–)39.6–52.8(–73.2)	46.0–68.0	40.0–60.0	45.0–80.0	46.0–65.0	65.0–91.0	49.8–59.4	42.0–50.0	39.6–49.5	50.0–58.0	29.7–66.0

vealed a suite of morphological diagnostic characteristics congruent with the characterization of the genus *Lithophyllum* Philippi (1837), and these characteristics were stated as follows: (1) non-parasitic thalli; (2) lack of genicula; (3) dorsiventral thalli organization; (4) presence of secondary pit connections and absence of cell fusions between the cells of adjacent filaments; (5) rounded or flattened epithallial cells; (6) length of subepithallial initial cells as long or longer compared to cells immediately subtending them; (7) uniporate conceptacles; (8) only unbranched spermatangial filaments were in a single conceptacle and spermatangia formation only on floors of male conceptacle chambers; (9) mature carposporangia terminated several-celled gonimoblast filaments that arise from a central fusion cell (Woelkerling, 1988; Woelkerling and Campbell, 1992; Harvey and Woelkerling, 2007; Xia, 2004; Basso et al., 2014).

Based on the morpho-anatomical analyses, thalli of *L. okamurae* were dorsiventral orientation crusts which consisted of three parts. The cells of the adjacent filaments of *L. okamurae* were connected only by secondary pit-connections, and the four types of conceptacles of *L. okamurae* were all uniporate. The morpho-anatomical characteristics of *L. okamurae*, which was firstly reported in the Sanya Bay, China, were in accordance with that previously described by Xia (2004). The sexual reproduction tissues were firstly described in this study which has not been described by Xia (2004). The characteristics of *L. okamurae* in comparison with species of the genus *Lithophyllum* were listed in Table 2. Various differences were observed among *L. okamurae* and the other reported species in genus *Lithophyllum*. For example, the epithallial cells of *L. okamurae* were square or rectangular in shape, and the peripheral regions were composed of square or elongated rectangular cells, which varied with that of the reported species of genus *Lithophyllum* (Table 2). In addition, the asexual conceptacles of *L. okamurae* were smaller than that of *L. atlanticum* from Brazil, but they were relatively larger than that of the other *Lithophyllum* species which were listed in Table 2 (Chamberlain, 1996; Vieira-Pinto et al., 2014; Xia, 2004). The spermatangial conceptacles of *L. okamurae* were relatively smaller than that of *L. incrassatum* (Chamberlain, 1996) and larger than that of *L. corallinae* (Xia, 2004). The carposporangial conceptacles of *L. okamurae* were relatively larger than that of *L. corallinae* (Xia, 2004). In this study, periodically synchronous epithallial shedding of *L. okamurae* was observed. Thus the attachment and growth of other reef organisms which adhered on this alga might be inhibited, which might bring implications to reef community structure (Keats et al., 1997; Pueschel and Keats, 1997; Nylund and Pavia, 2005; da Gama et al., 2014). The color of the conceptacles was translucent or white, which might indicate that the sporangia or carposporangia of *L. okamurae* were translucent. Therefore, DNA sequencing of *L. okamurae* was needed in order to clarify the species boundaries between the closely related populations.

DNA-based phylogenies have been widely applied in phylogenetic reconstructions of the species in subfamily Lithophylloideae (Vieira-Pinto et al., 2014; Basso et al., 2015; Hernández-Kantún et al., 2015, 2016; Pezzolesi et al., 2017; Richards et al., 2014, 2018; Torrano-Silva et al., 2018), and this molecular method was hypothesized to reveal additional undescribed species of genus *Lithophyllum* (Hernández-Kantún et al., 2016). However, none of the molecular researches had included the species of *L. okamurae* till now. In this study, the divergence values of 0.4%–6.1% in the 18S rDNA analyses, 7.1%–14.6% in the COI analyses, 6.6%–15.7% in the *rbc*L analyses and 2.6%–12.6% in the *psb*A analyses among *L. okamurae* and the other species of genus *Lithophyllum* provided molecular evidence to distinguish *L. okamurae* as a new species. The topology and branch pattern of the phylogenetic trees based on the four markers showed much degree of similarities with the topology of the phylogenetic trees in previous articles (Vieira-Pinto et al., 2014; Basso et al., 2015; Hernández-Kantún et al., 2015, 2016; Pezzolesi et al., 2017; Richards et al., 2014, 2018; Torrano-Silva et al., 2018). Based on the 18S rDNA phylogram results, individual of *L. okamurae* comprised a monophyletic lineage, which was closely related to the clade consisting of *L. atlanticum* (Brazil) and *L. margaritae* (Mexico) (ML distance value=96%, posterior probability=1), and remotely related to the other clades. In the COI tree, individual of *L. okamurae* comprised a monophyletic lineage, which was highly allied to the clade consisting of *Lithophyllum* sp. LAF7219 (Panama) (ML distance value=96%, posterior probability=1), and remotely related to the other clades. The *rbc*L tree shown that *L. okamurae* comprised a monophyletic lineage and was highly allied to the clade consisting of *L. atlanticum* (Brazil) (ML distance value=95%, posterior probability=1), and it was remotely related to the other clades. Based on the *psb*A phylogram results, individual of *L. okamurae* comprised a monophyletic lineage, which was closely related to the clade consisting of *Lithophyllum* sp. LAF7219 (Panama) (ML distance value=94%, posterior probability=1), and remotely related to the other clades. In general, *L. okamurae* was separated from the species in genus *Lithophyllum*, critical assessment of *L. okamurae* as a valid species could be made with confidence.

In conclusion, the morpho-anatomical characteristics of *L. okamurae* were firstly described in detail, and phylogenetic analyses based on four gene sequence datasets were also deeply studied in this study. Given the apparent instability of many diagnostic features used for species delimitation in genus *Lithophyllum*, the following combination of characters as reliable diagnostic characters for *L. okamurae* was proposed: (1) growth form encrusting to warty to lumpy; (2) 1 to 3 layer of epithallial cells rounded to flattened in section with polygonal, thick-walled cells in surface view; (3) palisade cells present; (4) spermatangial conceptacles (123.0–) 138.0–163.0 (–175.0) μm × (38.0–) 53.0–63.0 (–80.0) μm; (5) cystocarpic conceptacles (159.6–) 167.5–201.5 (–223) μm × 82.0–112.0 (–131.0) μm; (6) asexual conceptacles (170.0–) 240.0–265.0 (–315.0) μm × (100.0–) 125.0–150.0 μm. The species of *L. okamurae* was critically assessed as a valid species, and the closest clades of it were the clade consisting of *L. atlanticum* (Brazil) and *L. margaritae* (Mexico) and the clade consisting of *Lithophyllum* sp. LAF7219 (Panama). *L. okamurae* was remotely related to the other clades of genus *Lithophyllum*. Given the indispensable importance and ecological functions of the calcifying algae, it is necessary to investigate species diversity within the Lithophylloideae to provide theoretical basis for algae resources utilization and conservation in marine ecosystems.

References

Adey W H, Adey P J. 1973. Studies on the biosystematics and ecology of the epilithic crustose Corallinaceae of the British Isles. British Phycological Journal, 8(4): 343–407, doi: 10.1080/00071617300650381

Adey W H, Hernandez-Kantun J J, Johnson G, et al. 2015. DNA sequencing, anatomy, and calcification patterns support a monophyletic, subarctic, carbonate reef-forming *Clathromorphum* (Hapalidiaceae, Corallinales, Rhodophyta). Journal of Phycology, 51(1): 189–203, doi: 10.1111/jpy.12266

Basso D, Caragnano A, Le Gall L, et al. 2015. The genus *Lithophyllum* in the north-western Indian Ocean, with description of *L. yemenense* sp. nov., *L. socotraense* sp. nov., *L. subplicatum* comb.

et stat. nov., and the resumed *L. affine*, *L. kaiseri*, and *L. subreduncum* (Rhodophyta, Corallinales). Phytotaxa, 208(3): 183–200, doi: 10.11646/phytotaxa.208.3.1

Basso D, Caragnano A, Rodondi G. 2014. Trichocytes in *Lithophyllum kotschyanum* and *Lithophyllum* spp. (Corallinales, Rhodophyta) from the NW Indian Ocean. Journal of Phycology, 50(4): 711–717, doi: 10.1111/jpy.12197

Basso D, Rodondi G. 2006. A Mediterranean population of *Spongites fruticulosus* (Rhodophyta, Corallinales), the type species of Spongites, and the taxonomic status of *S. stalactitica* and *S. racemosa*. Phycologia, 45(4): 403–416, doi: 10.2216/04-93.1

Basso D, Rodondi G, Mari M. 2004. A comparative study between *Lithothamnion minervae* and the type material of *Millepora fasciculata* (Corallinales, Rhodophyta). Phycologia, 43(2): 215–223, doi: 10.2216/i0031-8884-43-2-215.1

Braga J C, Aguirre J. 2004. Coralline algae indicate Pleistocene evolution from deep, open platform to outer barrier reef environments in the northern Great Barrier Reef margin. Coral Reefs, 23(4): 547–558

Chamberlain Y M. 1996. Lithophylloid Corallinaceae (Rhodophyta) of the genera *Lithophyllum* and *Titanoderma* from southern Africa. Phycologia, 35(3): 204–221, doi: 10.2216/i0031-8884-35-3-204.1

Chihara M. 1974. The significance of reproductive and spore germination characteristics to the systematic of the Corallinaceae: nonarticulated coralline algae. Journal of Phycology, 10(3): 266–274

Clarkston B E, Saunders G W. 2010. A comparison of two DNA barcode markers for species discrimination in the red algal family Kallymeniaceae (Gigartinales, Florideophyceae), with a description of *Euthora timburtonii* sp. nov. Botany, 88(2): 119–131, doi: 10.1139/B09-101

da Gama B A P, Plouguerné E, Pereira R C. 2014. The antifouling defence mechanisms of marine macroalgae. Advances in Botanical Research, 71: 413–440, doi: 10.1016/B978-0-12-408062-1.00014-7

Ding Lanping, Huang Bingxin, Wang Hongwei. 2015. New classification system of marine red algae of China. Guangxi Sciences (in Chinese), 22(2): 164–188

Drummond A J, Rambaut A, Shapiro B, et al. 2005. Bayesian coalescent inference of past population dynamics from molecular sequences. Molecular Biology and Evolution, 22(5): 1185–1192, doi: 10.1093/molbev/msi103

Guiry M D, Guiry G M. 2018. AlgaeBase. World-wide electronic publication, National University of Ireland, Galway. http://www.algaebase.org [2016-08-27/2018-12-13]

Hajibabaei M, Singer G A C, Hebert P D N, et al. 2007. DNA barcoding: how it complements taxonomy, molecular phylogenetics and population genetics. Trends in Genetics, 23(4): 167–172, doi: 10.1016/j.tig.2007.02.001

Hall T A. 1999. BioEdit: a user-friendly biological sequence alignment editor and analysis program for Windows 95/98/NT. Nucleic Acids Symposium Series, 41: 95–98

Harper J T, Saunders G W. 2001. The application of sequences of the ribosomal cistron to the systematics and classification of the Florideophyte red algae (Florideophyceae, Rhodophyta). Cahiers de Biologie Marine, 42(1): 25–38

Harvey A S, Phillips L E, Woelkerling W J, et al. 2006. The Corallinaceae, subfamily Mastophoroideae (Corallinales, Rhodophyta) in south-eastern Australia. Australian Systematic Botany, 19(5): 387–429, doi: 10.1071/SB05029

Harvey A, Woelkerling W J. 2007. A guide to nongeniculate coralline red algal (Corallinales, Rhodophyta) rhodolith identification. Ciencias Marinas, 33(4): 411–426, doi: 10.7773/cm.v33i4.1210

Hernández-Kantún J J, Gabrielson P, Hughey J R, et al. 2016. Reassessment of branched *Lithophyllum* spp. (Corallinales, Rhodophyta) in the Caribbean Sea with global implications. Phycologia, 55(6): 619–639, doi: 10.2216/16-7.1

Hernández-Kantún J J, Rindi F, Adey W H, et al. 2015. Sequencing type material resolves the identity and distribution of the generitype *Lithophyllum incrustans*, and related European species *L. bathyporum* (Corallinales, Rhodophyta). Journal of Phycology, 51(4): 791–807, doi: 10.1111/jpy.12319

Johansen H W. 1976. Current status of generic concepts in coralline algae (Rhodophyta). Phycologia, 15(2): 221–244, doi: 10.2216/i0031-8884-15-2-221.1

Keats D W, Knight M A, Pueschel C M. 1997. Antifouling effects of epithallial shedding in three crustose coralline algae (Rhodophyta, Coralinales) on a coral reef. Journal of Experimental Marine Biology and Ecology, 213(2): 281–293, doi: 10.1016/S0022-0981(96)02771-2

Kundal P. 2011. Generic distinguishing characteristics and stratigraphic ranges of fossil corallines: an update. Journal of the Geological Society of India, 78(6): 571–586, doi: 10.1007/s12594-011-0119-z

Li Xiubao, Titlyanova T V, Titlyanov E A, et al. 2018. Coral Reef Marine Plants of Hainan Island (in Chinese). Beijing: Science Press, 1–242

Liu L C, Lin S M, Caragnano A, et al. 2018. Species diversity and molecular phylogeny of non-geniculate coralline algae (Corallinophycidae, Rhodophyta) from Taoyuan algal reefs in northern Taiwan, including *Crustaphytum* gen. nov. and three new species. Journal of Applied Phycology, 30(6): 3455–3469, doi: 10.1007/s10811-018-1620-1

Maggs C A, Verbruggen H, De Clerck O. 2007. Molecular systematics of red algae: building future structures on firm foundations. In: Brodie J, Lewis J, eds. Unravelling the Algae: The Past, Present, and Future of Algal Systematics. The Systematics Association Special Volume Series. Boca Raton, FL: CRC Press, 103–121

Maneveldt G W, Chamberlain Y M, Keats D W. 2008. A catalogue with keys to the non-geniculate coralline algae (Corallinales, Rhodophyta) of South Africa. South African Journal of Botany, 74(4): 555–566, doi: 10.1016/j.sajb.2008.02.002

McCoy S J, Kamenos N A. 2015. Coralline algae (Rhodophyta) in a changing world: integrating ecological, physiological, and geochemical responses to global change. Journal of Phycology, 51(1): 6–24, doi: 10.1111/jpy.12262

Nelson W A. 2009. Calcified macroalgae-critical to coastal ecosystems and vulnerable to change: a review. Marine and Freshwater Research, 60(8): 787–801, doi: 10.1071/MF08335

Nelson W A, Sutherland J E, Farr T J, et al. 2015. Multi-gene phylogenetic analyses of New Zealand coralline algae: *Corallinapetra novaezelandiae* gen. et sp. nov. and recognition of the Hapalidiales ord. nov. Journal of Phycology, 51(3): 454–468, doi: 10.1111/jpy.12288

Nylander J A A. 2004. MrModeltest v2. Program distributed by the author. Uppsala: Evolutionary Biology Centre, Uppsala University

Nylund G M, Pavia H. 2005. Chemical versus mechanical inhibition of fouling in the red alga *Dilsea carnosa*. Marine Ecology Progress Series, 299: 111–121, doi: 10.3354/meps299111

Peña V, Hernandez-Kantun J J, Adey W H, et al. 2018. Assessment of coralline species diversity in the European coasts supported by sequencing of type material: the case study of *Lithophyllum nitorum* (Corallinales, Rhodophyta). Cryptogamie, Algologie, 39(1): 123–137, doi: 10.7872/crya/v39.iss1.2018.123

Pezzolesi L, Falace A, Kaleb S, et al. 2017. Genetic and morphological variation in an ecosystem engineer, *Lithophyllum byssoides* (Corallinales, Rhodophyta). Journal of Phycology, 53(1): 146–160, doi: 10.1111/jpy.12488

Phang S M, Yeong H Y, Ganzon-Fortes E T, et al. 2016. Marine algae of the South China Sea bordered by Indonesia, Malaysia, Philippines, Singapore, Thailand and Vietnam. Raffles Bulletin of Zoology Supplement, 34: 13–59

Pueschel C M, Keats D W. 1997. Fine structure of deep-layer sloughing and epithallial regeneration in *Lithophyllum neoatalayense* (Corallinales, Rhodophyta). Phycological Research, 45(1): 1–8, doi: 10.1111/j.1440-1835.1997.tb00056.x

Richards J L, Gabrielson P W, Fredericq S. 2014. New insights into the genus *Lithophyllum* (Lithophylloideae, Corallinaceae, Corallinales) from deepwater rhodolith beds offshore the NW Gulf of Mexico. Phytotaxa, 190(1): 162–175, doi: 10.11646/phytotaxa.190.1.11

Richards J L, Gabrielson P W, Hughey J R, et al. 2018. A re-evaluation of subtidal *Lithophyllum* species (Corallinales, Rhodophyta) from North Carolina, USA, and the proposal of *L. searlesii* sp. nov. Phycologia, 57(3): 318–330, doi: 10.2216/17-110.1

Riosmena-Rodríguez R, Nelson W, Aguirre J. 2017. Rhodolith/Maërl Beds: A Global Perspective. Cham: Springer, 2–362

Riosmena-Rodríguez R, Woelkerling W J, Foster M S. 1999. Taxonomic reassessment of rhodolith-forming species of *Lithophyllum* (Corallinales, Rhodophyta) in the Gulf of California, Mexico. Phycologia, 38(5): 401–417, doi: 10.2216/i0031-8884-38-5-401.1

Rösler A, Perfectti F, Peña V, et al. 2016. Phylogenetic relationships of Corallinaceae (Corallinales, Rhodophyta): taxonomic implications for reef-building corallines. Journal of Phycology, 52(3): 412–431, doi: 10.1111/jpy.12404

Saunders G W. 2005. Applying DNA barcoding to red macroalgae: a preliminary appraisal holds promise for future applications. Philosophical Transactions of the Royal Society B: Biological Sciences, 360(1462): 1879–1888, doi: 10.1098/rstb.2005.1719

Steneck R S. 1986. The ecology of coralline algal crusts: convergent patterns and adaptative strategies. Annual Review of Ecology and Systematics, 17: 273–303, doi: 10.1146/annurev.es.17.110186.001421

Tamura K, Peterson D, Peterson N, et al. 2011. MEGA5: molecular evolutionary genetics analysis using maximum likelihood, evolutionary distance, and maximum parsimony methods. Molecular Biology and Evolution, 28(10): 2731–2739, doi: 10.1093/molbev/msr121

Torrano-Silva B N, Vieira B R, Riosmena-Rodríguez R, et al. 2018. Guidelines for DNA barcoding of coralline algae, focusing on Lithophylloideae (Corallinales) from Brazil. Botanica Marina, 61(2): 127–140, doi: 10.1515/bot-2017-0040

van der Heijden L H, Kamenos N A. 2015. Reviews and syntheses: calculating the global contribution of coralline algae to total carbon burial. Biogeosciences, 12(21): 6429–6441, doi: 10.5194/bg-12-6429-2015

Verlaque M. 2010. Field-methods to analyse the condition of Mediterranean *Lithophyllum byssoides* (Lamarck) Foslie rims. Scientific Reports of Port-Cros National Park, 24: 185–196

Vidal R, Meneses I, Smith M. 2003. Molecular genetic identification of crustose representatives of the order Corallinales (Rhodophyta) in Chile. Molecular Phylogenetics and Evolution, 28(3): 404–419, doi: 10.1016/S1055-7903(03)00123-4

Vieira-Pinto T, Oliveira M C, Bouzon J, et al. 2014. *Lithophyllum* species from Brazilian coast: range extension of *Lithophyllum margaritae* and description of *Lithophyllum atlanticum* sp. nov. (Corallinales, Corallinophycidae, Rhodophyta). Phytotaxa, 190(1): 355–369, doi: 10.11646/phytotaxa.190.1.21

Villas-Boas A B, Riosmena-Rodríguez R, Amado-Filho G M, et al. 2009. Rhodolith-forming species of *Lithophyllum* (Corallinales; Rhodophyta) from Espírito Santo State, Brazil, including the description of *L. depressum* sp. nov. Phycologia, 48(4): 237–248, doi: 10.2216/08-35.1

Woelkerling W J. 1983. A taxonomic reassessment of *Lithothamnium* (Corallinaceae, Rhodophyta) based on studies of R. A. Philippi' s original collections. British Phycological Journal, 18(2): 165–197, doi: 10.1080/00071618300650211

Woelkerling W J. 1988. The Coralline Red Algae: An Analysis of the Genera and Subfamilies of Nongeniculate Corallinaceae. Oxford, New York: Oxford University Press, 1–268

Woelkerling W J. 1996. Subfamily lithophylloideae. In: Womersley H B S, ed. The Marine Benthic Flora of Southern Australia. Part IIIB. Gracilariales, Rhodymeniales, Corallinales and Bonnemaisoniales. Canberra: Australian Biological Resources Study, 214–237

Woelkerling W J, Campbell S J. 1992. An account of southern Australian species of *Lithophyllum* (Corallinaceae, Rhodophyta). Bulletin of the British Museum of (Natural History) Botany Series, 22(1): 1–107

Woelkerling W J, Gustavsen G, Myklebost H E, et al. 2005. The coralline red algal herbarium of Mikael Foslie: revised catalogue with analyses. Gunneria, 77: 1–625

Woelkerling W J, Irvine L M, Harvey A S. 1993. Growth-forms in non-geniculate coralline red algae (Corallinales, Rhodophyta). Australian Systematic Botany, 6(4): 277–293, doi: 10.1071/SB9930277

Xia Bangmei. 2004. Flora Algarum Marinarum Sinicarum Tomus II Rhodophyta No. IV Corallinales (in Chinese). Beijing: Science Press, 1–147

Yoon H S, Hackett J D, Bhattacharya D. 2002. A single origin of the peridinin- and fucoxanthin-containing plastids in dinoflagellates through tertiary endosymbiosis. Proceedings of the National Academy of Sciences of the United States of America, 99(18): 11724–11729, doi: 10.1073/pnas.172234799

Supplementary information:

Fig. S1. Tree constructed with ML for the COI alignment. Values at branches represent distance analyses of 1 000 bootstrap replicates (left value) and Bayesian posterior probabilities (right value). Branches lacking values received <50% support. GenBank accession numbers provided. The newly generated sequence was shown in bold.

Fig. S2. Tree constructed with ML for the *psb*A alignment. Values at branches represent distance analyses of 1 000 bootstrap replicates (left value) and Bayesian posterior probabilities (right value). Branches lacking values received <50% support. GenBank accession numbers provided. The newly generated sequence was shown in bold.

Fig. S3. Tree constructed with BA for the 18R rDNA alignment. Values at branches indicate Bayesian posterior probabilities. Branches lacking values received <0.5 support. GenBank accession numbers provided. The newly generated sequence was shown in bold.

Fig. S4. Tree constructed with BA for the COI alignment. Values at branches indicate Bayesian posterior probabilities. Branches lacking values received <0.5 support. GenBank accession numbers provided. The newly generated sequence was shown in bold.

Fig. S5. Tree constructed with BA for the *rbc*L alignment. Values at branches indicate Bayesian posterior probabilities. Branches lacking values received <0.5 support. GenBank accession numbers provided. The newly generated sequence was shown in bold.

Fig. S6. Tree constructed with BA for the *psb*A alignment. Values at branches indicate Bayesian posterior probabilities. Branches lacking values received <0.5 support. GenBank accession numbers provided. The newly generated sequence was shown in bold.

The supplementary information is available online at https://doi.org/10.1007/s13131-019-1470-y. The supplementary information is published as submitted, without typesetting or editing. The responsibility for scientific accuracy and content remains entirely with the authors.